Journal of
Materials Chemistry C

PAPER

View Article Online
View Journal | View Issue

Check for updates

Cite this: J. Mater. Chem. C, 2018, 6, 12001

Electron transport at the interface of organic semiconductors and hydroxyl-containing dielectrics†

Huihong Jiang, Zhuoting Huang, Guobiao Xue, Hongzheng Chen and Hanying Li *

Received 20th March 2018,
Accepted 23rd April 2018

DOI: 10.1039/c8tc01343h

rsc.li/materials-c

Dielectric material design is challenging for the fabrication of n-channel organic field-effect transistors (OFETs). Hydroxyl groups in dielectrics have been found to intensively trap electrons and completely eliminate electron transport in a variety of structurally disordered organic semiconductors, which generally excludes the widely used hydroxyl-containing dielectrics from n-channel OFETs. Here, we show that electrons are clearly more mobile at the interface of organic semiconductors and hydroxyl-containing dielectrics, including silica, polyvinyl alcohol (PVA) and poly(4-vinyl phenol) (PVP), when single-crystalline C_{60} or 6,13-bis(triisopropylsilylethynyl)pentacene (TIPS-pentacene) are used as semiconductors in OFETs. With regards to C_{60}, an electron mobility larger than 1 $cm^2 V^{-1} s^{-1}$ has been achieved, indicating that the hydroxyl groups have a limited trapping effect on electron transport. Electron trapping becomes more intensive either by exposing the dielectric/device to air or by increasing the hydroxyl density in the dielectrics, suggesting that the trapping effect is associated with water absorbed by the dielectrics. By showing their limited negative effect, this work suggests that the widely used, easily accessible and well-known hydroxyl groups might be incorporated into organic electronic materials for n-channel OFETs and complementary circuits fabricated in a glove box.

Introduction

Charge transport in organic semiconductors is a basic electronic property that is critical for all kinds of organic electronic devices including organic field-effect transistors (OFETs),[1–4] solar cells,[5–8] and light-emitting diodes.[9–12] Electron and hole transport are equally important for both fundamental studies and applications for double-carrier electronic devices.[5–13] However, experimental results based on the transport measurement for OFETs generally show that electron transport is more difficult to achieve than hole transport, in terms of mobility and the variety of materials exhibiting high mobility.[2–4,14–22] This disparity is often attributed to the extrinsic factors that are detrimental to electron transport and mask the intrinsic electron mobility.[23–27] One of the major factors is widely recognized as the electron traps associated with hydroxyl groups. Chua *et al.*[24] achieved significant electron mobility in various conjugated polymers including poly(fluorene), poly(*p*-phenylenevinylene), and poly(thiophene) coated on hydroxyl-free gate dielectrics. In sharp contrast, electron transport was not observed when the dielectric was replaced with the commonly used silica, in the form of silanol, which contains hydroxyl groups. Aided by spectrometry, the hydroxyl groups were identified to be a source of electron traps through an electrochemical mechanism. Since then, the notion that hydroxyl groups have a negative effect on electron transport has been widely held. Hydroxyl-containing dielectrics (*e.g.* poly(4-vinyl phenol) (PVP)) are not typically considered for n-channel OFETs, although they are widely used for high-performance p-channel OFETs and have exhibited advantages such as high dielectric constants.[28] Interestingly, polyvinyl alcohol (PVA), which is rich in hydroxyl groups, has been occasionally used as a dielectric layer for OFETs based on typical p-channel materials, such as pentacene and TIPS-pentacene, by various research groups and these devices showed weak but clear n-channel conduction with electron mobilities up to 0.2 $cm^2 V^{-1} s^{-1}$.[28–32] The discrepancy of the hydroxyl effect on n-channel OFETs might be due to the different semiconductors or dielectrics and this encourages the revisiting of the hydroxyl effect on electron transport, which is not clear.

Previous studies associated with the hydroxyl effect are mostly based on polycrystalline or amorphous organic semiconductors. The charge transport in these relatively disordered materials is disorder-limited.[33] Ideally, the hydroxyl effect should be reflected better in single-crystalline organic semiconductors.

MOE Key Laboratory of Macromolecule Synthesis and Functionalization, State Key Laboratory of Silicon Materials, Department of Polymer Science and Engineering, Zhejiang University, Hangzhou, 310027, P. R. China. E-mail: hanying_li@zju.edu.cn

† Electronic supplementary information (ESI) available. See DOI: 10.1039/c8tc01343h

Published on 23 April 2018. Downloaded by Fail Open on 7/05/2025 9:23:25 PG.

Published on 23 April 2018. Downloaded by Fail Open on 7/05/2025 9:23:25 PG.

In this work, we examine this effect by interfacing the hydroxyl rich dielectrics with organic single crystals instead of disordered materials. We observe remarkable electron transport at the interfaces and demonstrate that the electron-trap effects in these ordered materials are limited for the single-crystalline organic semiconductors, C_{60} and TIPS-pentacene.

Results and discussion

C_{60}, as an outstanding electronic material,[34,35] was selected as the semiconducting layer, while PVA (24–32 nm) or PVP (24–25 nm) coated on 300 nm SiO_2 were selected as the dielectric layers to construct OFETs in order to study the hydroxyl effect on electron transport in an OFET configuration (Fig. 1a). On the semiconductor side, C_{60} forms, from solution, well-aligned long single-crystal ribbons[36,37] (Fig. 1c–f) that facilitate OFET fabrication. On the dielectric side, PVA and PVP, with their molecular structures shown in Fig. 1b, are widely used as dielectric materials for p-channel OFETs[38–43] and these polymers both contain high-density hydroxyl groups. PVP has one hydroxyl group in each repeating unit, while the PVA used here has a degree of hydrolysis of 80% (PVA-80), and contains one hydroxyl group in about 80% of repeating units.

Well-aligned C_{60} single crystal ribbons were interfaced onto the hydroxyl-containing polymer films by growing the crystals using the drop-pinned crystallization (DPC) method[36,44] in a N_2 glove box to reduce the effect of water moisture, which is detrimental to electron transport.[25] Similar to a previous report,[36] the obtained crystals on both polymer surfaces were several hundred microns long, 5–10 μm wide and 55–70 nm thick, with a smooth single-crystalline terrace (rms roughness ~0.4 nm).

Next, OFETs with a top-contact, bottom-gate configuration were constructed by depositing a 90 nm Ag source and drain electrodes perpendicular to the aligned crystals.

The performance of the OFETs was measured in a N_2 glove box. Interestingly, the electron is clearly mobile on both PVA-80% and PVP dielectrics, as shown by the typical transfer (Fig. 2a and d) and output characteristics (Fig. 2b and e). The electron mobility, on to off current ratios (I_{on}/I_{off}) and threshold voltages (V_T) were extracted (Table 1) and histograms of the electron mobility for 50 devices from 6 substrates are shown in Fig. 2c and f. The average electron mobility of the PVA-80% dielectric OFET device is 1.46 ± 0.57 $cm^2 V^{-1} s^{-1}$ (ranging from 0.51 to 2.86 $cm^2 V^{-1} s^{-1}$) and the average electron mobility of the PVP dielectric OFET device reached a comparable value of 1.22 ± 0.37 $cm^2 V^{-1} s^{-1}$ (ranging from 0.53 to 1.86 $cm^2 V^{-1} s^{-1}$).

For comparison, two control experiments were performed. First, a hydroxyl-free polymer, BCB, which has been demonstrated to be an excellent dielectric[24] was also used for OFETs, as reported in the previous paper.[36] The characteristics of the OFET devices with the BCB dielectric are shown in Fig. S1(a–c) (ESI†). The average electron mobility was 2.29 ± 0.98 $cm^2 V^{-1} s^{-1}$ (ranging from 0.51 to 5.51 $cm^2 V^{-1} s^{-1}$). Second, SiO_2 without

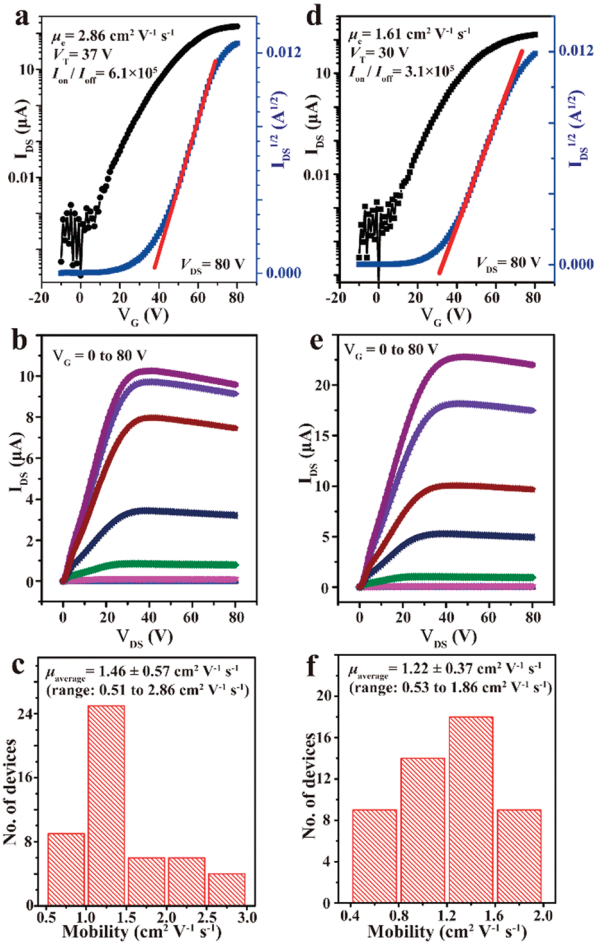

Fig. 2 OFET characteristics of C_{60} single crystals grown on PVA-80% (a–c) and PVP (d–f). (a and d) Typical transfer characteristics. (b and e) Typical output characteristics. (c and f) Histograms of the electron mobility for 50 devices.

Table 1 OFET parameters for C_{60} devices on various dielectric layers

Dielectrics	Electron mobility ($cm^2 V^{-1} s^{-1}$)	I_{on}/I_{off}	V_T (V)	ΔV_T (V) from hysteresis
PVA-80%	1.46 ± 0.57	~10^4	33–44	5 ± 2
PVP	1.22 ± 0.37	~10^4	34–49	13 ± 2
BCB	2.29 ± 0.98	~10^4	27–53	3 ± 1
SiO_2	1.70 ± 0.84	~10^4	23–48	10 ± 2

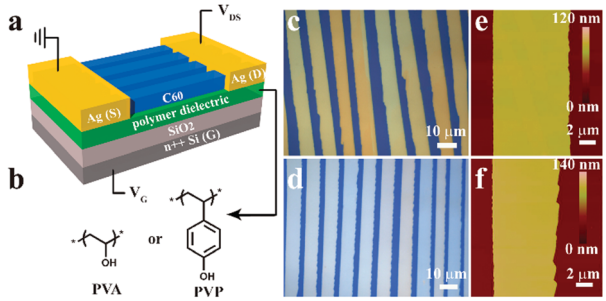

Fig. 1 (a) The configuration of the OFETs, where S represents source, D is drain and G is gate. (b) The molecular structures of the polymer dielectrics. (c–f) The morphology of C_{60} single crystals grown on PVA-80% (c and e) and PVP films (d and f): (c and d) OM images of the crystals; (e and f) AFM images of the crystals.

 This journal is © The Royal Society of Chemistry 2018

Published on 23 April 2018. Downloaded by Fail Open on 7/05/2025 9:23:25 PG.

any polymer coating was used as the dielectric. The density of the hydroxyl groups on the pristine wafer with dry thermal SiO_2 was large enough to eliminate electron transport in a variety of polymer films, as shown in ref. 24. However, in the case of the C_{60} single crystal ribbons examined here, electron transport was not eliminated and the average electron mobility reached 1.70 ± 0.84 cm^2 V^{-1} s^{-1} (ranging from 0.55 to 3.98 cm^2 V^{-1} s^{-1}) (Fig. S1(d–f), ESI†).

The electron transport properties based on the four different dielectrics show that the C_{60} devices exhibit an electron mobility of more than 1 cm^2 V^{-1} s^{-1}, both on hydroxyl-containing and hydroxyl-free dielectrics, indicating that hydroxyl groups have a limited trapping effect on electron transport. This effect is not intensive enough to completely eliminate electron transport in the C_{60} single crystal. However, it slightly reduces the electron mobility and the OFETs that are based on hydroxyl-containing dielectrics exhibit lower mobility than those based on the hydroxyl-free BCB dielectric. This slight trapping effect can be seen from the V_T shift (ΔV_T) measured from the transfer hysteresis on the four dielectrics (Table 1 and Fig. S2, ESI†). Clearly, ΔV_T for the hydroxyl-containing dielectrics is larger than that for the hydroxyl-free BCB dielectric, which is indicative of a higher trap density.[45–47]

Next, we examined electron transport at the interface of another organic semiconductor, TIPS-pentacene,[48] and the PVP dielectric. Similar conductive channels have previously been examined based on either polycrystalline pentacene or single-crystalline TIPS-pentacene.[28–30] No n-channel behavior was observed even if low-work-function Ca electrodes were used for electron injection.[28] We revisited the properties of the channels formed by PVP and TIPS-pentacene single-crystal ribbons (Fig. S3a–c, ESI†),[49,50] avoiding the exposure of the devices to air by fabricating the devices in a N_2 glove box. To our surprise, the devices showed clear electron transport from the transfer and output characteristics using Ag (Fig. 3) or Au (Fig. S4, ESI†) electrodes. A histogram of the electron mobility for 50 devices from 4 substrates is shown in Fig. 3c. With regards to electron transport, an electron mobility ranging from 3.67×10^{-4} to 0.20 cm^2 V^{-1} s^{-1}, an $I_{on}/I_{off} > 10^1$, and a V_T between 68 and 101 V were obtained. The wide range of mobility and high V_T suggest poor electron injection, however, every device shows n-channel behavior, indicating that the electron

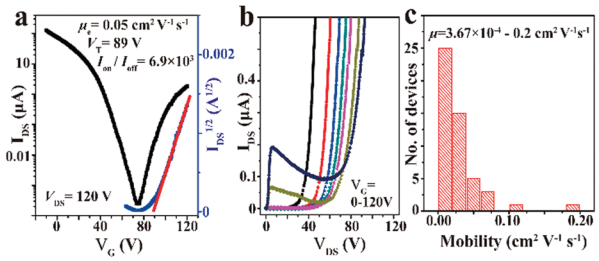

Fig. 3 OFET characteristics of TIPS-pentacene single crystals grown on PVP, using Ag as the electrode. (a) Typical transfer characteristics of the OFETs in n-channel operation mode. (b) Typical output characteristics of the OFETs in n-channel operation mode. (c) A histogram of the electron mobility of 50 devices.

Table 2 OFET parameters for C_{60} devices on three types of PVA dielectric layers

Polymer dielectrics	Electron mobility (cm^2 V^{-1} s^{-1})	I_{on}/I_{off}	V_T (V)
PVA-80%	1.46 ± 0.57	$\sim 10^4$	33–44
PVA-87–89%	0.85 ± 0.19	$\sim 10^4$	8–36
PVA-99+%	0.52 ± 0.17	$\sim 10^4$	18–47

is also mobile at the semiconductor/dielectric interface. This result is consistent with the n-channel behavior observed at the polycrystalline-pentacene/PVA[28,29] and single-crystalline-TIPS-pentacene/PVA interfaces.[30]

The above observations of the n-channel behaviour are distinct from previous reports[28–30] on the effect of hydroxyl groups. Comparing the detailed experimental method reveals two differences between the previous and current work. On one hand, disordered (polycrystalline and amorphous) semiconductors were used previously while single-crystalline semiconductors are adopted here. On the other hand, more operations are kept in a N_2 atmosphere in the current work to avoid exposing the channels to air. These two differences imply that the hydroxyl groups do not act as electron traps independently but cooperatively with absorbed water. This implication is supported by the three pieces of evidence below. First, we chose three types of PVA with an increasing degree of hydrolysis (80%, 87–89% and 99+%) and thus, increasing concentrations of hydroxyl groups (one hydroxyl in about 80%, 87–89% and 99+% of the repeating units) as the dielectric layer for C_{60}-OFETs and observed that higher hydroxyl concentration resulted in significantly lower electron mobility (from 1.46 ± 0.57 cm^2 V^{-1} s^{-1} to 0.52 ± 0.17 cm^2 V^{-1} s^{-1}) (Table 2 and Fig. S6, ESI†). In addition, when these devices were then exposed to the atmosphere with $\sim$40% humidity for 24 h, the morphology of the crystals showed no obvious change (Fig. S7, ESI†) but the mobility decreased in all three cases by 28.5%, 35.4%, and 66.4%, respectively, and the devices with higher hydroxyl concentrations were degraded more severely (Fig. 4). Second, comparison of the performance of the C_{60} single crystal OFET devices on the SiO_2 dielectric fabricated

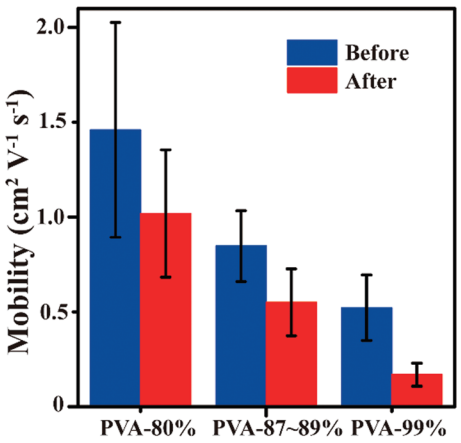

Fig. 4 The electron mobility change in the OFET devices based on three types of PVA dielectrics before and after exposing to air.

Published on 23 April 2018. Downloaded by Fail Open on 7/05/2025 9:23:25 PG.

in air (Fig. S8, ESI†) and in a N_2 glove box (Fig. S1d–f, ESI†) shows dramatically lowered mobility in the former (the former: 0.19 ± 0.10 $cm^2 V^{-1} s^{-1}$; the latter: 1.70 ± 0.84 $cm^2 V^{-1} s^{-1}$). Third, when the PVP-coated substrate was exposed to air for 3 days before crystallization of the TIPS-pentacene single crystals, the devices exhibited no electron transport but only p-channel behavior. Based on the above evidence, we attribute the effect of hydroxyl groups on electron transport in OFETs mainly to their hydrophilicity and their negative effect is limited in the absence of water molecules. This explanation is consistent with the reported negative effects of water, which is accommodated either by the polymer dielectrics[51] or polymer semiconductors.[52] Polycrystalline and amorphous materials have more defects (*e.g.*, grain boundaries), which may accommodate the absorbed water, as compared to single-crystalline materials. As such, the effect of hydroxyl groups is more accessible in the disordered materials.

Conclusions

In summary, we have revisited the hydroxyl effect on electron transport using single-crystalline organic semiconductors instead of disordered materials. In particular, this work demonstrates that hydroxyl groups at the interface of organic semiconductors and organic hydroxyl-containing dielectrics only have a limited trapping effect on electron transport and this negative effect is associated with the hydrophilicity of hydroxyl-containing dielectrics. Clear electron transport can be observed in OFETs when C_{60} and TIPS-pentacene single crystals are interfaced with PVA or PVP. An electron mobility above 1 $cm^2 V^{-1} s^{-1}$ has been achieved based on C_{60}. As such, this work suggests that the widely used hydroxyl-containing dielectrics may be applicable for n-channel OFETs and these common dielectric layers may be used for complementary circuits when the devices are fabricated in a glove box.

Experimental

Dielectric fabrication and characterization

PVA-80% (Aldrich, M_w = 9–10 kD, with a degree of hydrolysis of 80%), PVA-87–89% (Aldrich, M_w = 13–23 kD, with a degree of hydrolysis of 87–89%), PVA-99+% (Aldrich, M_w = 130 kD, with a degree of hydrolysis of 99+%) and PVP (Aldrich, M_w = 25 kD) were used as the polymer dielectrics. PVA-80% (10 mg mL^{-1} in deionized water) and PVP (10 mg mL^{-1} in *n*-butyl acetate) were spin-coated onto a SiO_2 (300 nm)/Si substrate at 2000 rpm. The spin-coating speed for PVA-87–89% (10 mg mL^{-1} in deionized water) and PVA-99+% (10 mg mL^{-1} in deionized water) was 4000 rpm. Then, the substrates that contained PVA were pretreated at 100 °C for 12 h in air, followed by baking at 100 °C for 12 h in a N_2 glove box. The PVP-coated substrates were spin-coated and baked at 50 °C for 12 h in a N_2 glove box. The thickness of these dielectrics was 24–25 nm for PVP, 24–27 nm for PVA-80%, 31–32 nm for PVA-87–89%, and 28–29 nm for PVA-99+%.

Crystal growth and characterization

C_{60} (Alfar Aesar) and TIPS-pentacene (Sigma-Aldrich) single crystals were grown on polymer dielectric-covered substrates using the DPC method in a N_2 glove box. In the case of the C_{60} crystals, a C_{60} solution (20 μL, 0.4 mg mL^{-1}), dissolved in a mixed solvent of carbon tetrachloride (CCl_4, Aladdin) and *m*-xylene (Sigma-Aldrich), with a volume ratio of 4 : 3, was dropped onto the substrates with a pinner (small piece of silicon wafer, 0.3 × 0.3 cm^2) at 30 ± 1 °C in a sealed environment (a Petri dish sealed by parafilm). Evaporation of the solvents resulted in well-aligned C_{60} single crystal ribbons with incorporated solvent molecules (*m*-xylene and CCl_4).[36] In the case of the TIPS-pentacene crystals, a similar procedure was adopted. A TIPS-pentacene solution (15 μL, 0.3 mg mL^{-1}), dissolved in hexane (TCI), was used and the substrate temperature was kept at 25 ± 1 °C. Similarly, well-aligned ribbon crystals were obtained. The morphology of the crystals was characterized using optical microscopy (OM, Nikon LV100 POL) and atomic force microscopy (AFM, Veeco 3D). The thickness of the polymer films was also measured using AFM.

Device fabrication and characterization

OFETs were fabricated by depositing source and drain electrodes (90 nm Ag), using a shadow mask with a channel length (L) of 50 μm and a width (W) of 1 mm in a top-contact, bottom-gate configuration. Since the crystals only partially covered the channel area, the real value of W/L was measured from the physical dimensions of the covered channel area.[36] The performance of the OFETs was measured using a Keithley4200 SCS semiconductor parameter analyzer in a glove box. The mobility was calculated from the saturation regime and it was reported as the mean ± SD. The capacitance per unit area (C_i) of the dielectrics was measured using a Keithley4200 SCS semiconductor parameter analyzer, with a C_i of 9.6, 10.7, 11.3 and 10.5 nF cm^{-2} for PVA-80%, PVA-87–89%, PVA-99+% and PVP, respectively, and they were coated onto 300 nm SiO_2.

Except for the weighing of the reagents and the preparation of the PVA dielectrics, all of the processes were performed in a N_2 glove box.

Conflicts of interest

There are no conflicts of interest to declare.

Acknowledgements

This work was supported by the 973 Program (2014CB643503) and the National Natural Science Foundation of China (51625304, 51461165301).

References

1 L. Shi, Y. Guo, W. Hu and Y. Liu, *Mater. Chem. Front.*, 2017, **1**, 2423–2456.
2 J. Dhar, U. Salzner and S. Patil, *J. Mater. Chem. C*, 2017, **5**, 7404–7430.
3 H. Sirringhaus, *Adv. Mater.*, 2014, **26**, 1319–1335.

 This journal is © The Royal Society of Chemistry 2018

Published on 23 April 2018. Downloaded by Fail Open on 7/05/2025 9:23:25 PG.

4 H. Dong, X. Fu, J. Liu, Z. Wang and W. Hu, *Adv. Mater.*, 2013, **25**, 6158–6183.
5 J. W. Jung, J. W. Jo, E. H. Jung and W. H. Jo, *Org. Electron.*, 2016, **31**, 149–170.
6 J. S. Manser, J. A. Christians and P. V. Kamat, *Chem. Rev.*, 2016, **116**, 12956–13008.
7 P. Cheng and X. Zhan, *Mater. Horiz.*, 2015, **2**, 462–485.
8 L. Lu, T. Zheng, Q. Wu, A. M. Schneider, D. Zhao and L. Yu, *Chem. Rev.*, 2015, **115**, 12666–12731.
9 C. Zhang, P. Chen and W. Hu, *Small*, 2016, **12**, 1252–1294.
10 J. Yang, J. Huang, Q. Li and Z. Li, *J. Mater. Chem. C*, 2016, **4**, 2663–2684.
11 J.-H. Jou, S. Kumar, A. Agrawal, T.-H. Li and S. Sahoo, *J. Mater. Chem. C*, 2015, **3**, 2974–3002.
12 H. Sasabe and J. Kido, *Chem. Mater.*, 2011, **23**, 621–630.
13 B. Crone, A. Dodabalapur, Y. Y. Lin, R. W. Filas, Z. Bao, A. LaDuca, R. Sarpeshkar, H. E. Katz and W. Li, *Nature*, 2000, **403**, 521.
14 J. E. Anthony, A. Facchetti, M. Heeney, S. R. Marder and X. Zhan, *Adv. Mater.*, 2010, **22**, 3876–3892.
15 Y. Zhao, Y. Guo and Y. Liu, *Adv. Mater.*, 2013, **25**, 5372–5391.
16 Y.-Q. Zheng, T. Lei, J.-H. Dou, X. Xia, J.-Y. Wang, C.-J. Liu and J. Pei, *Adv. Mater.*, 2016, **28**, 7213–7219.
17 X. Xu, Y. Yao, B. Shan, X. Gu, D. Liu, J. Liu, J. Xu, N. Zhao, W. Hu and Q. Miao, *Adv. Mater.*, 2016, **28**, 5276–5283.
18 G. Xue, J. Wu, C. Fan, S. Liu, Z. Huang, Y. Liu, B. Shan, H. L. Xin, Q. Miao, H. Chen and H. Li, *Mater. Horiz.*, 2016, **3**, 119–123.
19 H. Luo, C. Yu, Z. Liu, G. Zhang, H. Geng, Y. Yi, K. Broch, Y. Hu, A. Sadhanala, L. Jiang, P. Qi, Z. Cai, H. Sirringhaus and D. Zhang, *Sci. Adv.*, 2016, **2**, e1600076.
20 S. F. Yang, Z. T. Liu, Z. X. Cai, M. J. Dyson, N. Stingelin, W. Chen, H. J. Ju, G. X. Zhang and D. Q. Zhang, *Adv. Sci.*, 2017, **4**, 1700048.
21 X. Gao and Z. Zhao, *Sci. China: Chem.*, 2015, **58**, 947–968.
22 X. Zhao, G. Xue, G. Qu, V. Singhania, Y. Zhao, K. Butrouna, A. Gumyusenge, Y. Diao, K. R. Graham and H. Li, *Macromolecules*, 2017, **50**, 6202–6209.
23 J. Zaumseil and H. Sirringhaus, *Chem. Rev.*, 2007, **107**, 1296–1323.
24 L.-L. Chua, J. Zaumseil, J.-F. Chang, E. C. W. Ou, P. K. H. Ho, H. Sirringhaus and R. H. Friend, *Nature*, 2005, **434**, 194.
25 D. M. de Leeuw, M. M. J. Simenon, A. R. Brown and R. E. F. Einerhand, *Synth. Met.*, 1997, **87**, 53–59.
26 N. A. Minder, S. Ono, Z. Chen, A. Facchetti and A. F. Morpurgo, *Adv. Mater.*, 2012, **24**, 503–508.
27 H. Sirringhaus, *Nat. Mater.*, 2003, **2**, 641.
28 J.-W. Chang, W.-L. Hsu, C.-Y. Wu, T.-F. Guo and T.-C. Wen, *Org. Electron.*, 2010, **11**, 1613–1619.
29 T. B. Singh, F. Meghdadi, S. Günes, N. Marjanovic, G. Horowitz, P. Lang, S. Bauer and N. S. Sariciftci, *Adv. Mater.*, 2005, **17**, 2315–2320.
30 Z.-T. Huang, G.-B. Xue, J.-K. Wu, S. Liu, H.-B. Li, Y.-H. Yang, F. Yan, P. K. L. Chan, H.-Z. Chen and H.-Y. Li, *Chin. Chem. Lett.*, 2016, **27**, 1781–1787.
31 T. B. Singh, P. Senkarabacak, N. S. Sariciftci, A. Tanda, C. Lackner, R. Hagelauer and G. Horowitz, *Appl. Phys. Lett.*, 2006, **89**, 033512.
32 S. Takebayashi, S. Abe, K. Saiki and K. Ueno, *Appl. Phys. Lett.*, 2009, **94**, 083305.
33 V. Podzorov, *MRS Bull.*, 2013, **38**, 15–24.
34 X.-H. Zhang and B. Kippelen, *J. Appl. Phys.*, 2008, **104**, 104504.
35 T. D. Anthopoulos, B. Singh, N. Marjanovic, N. S. Sariciftci, A. M. Ramil, H. Sitter, M. Cölle and D. M. d. Leeuw, *Appl. Phys. Lett.*, 2006, **89**, 213504.
36 H. Li, B. C. K. Tee, J. J. Cha, Y. Cui, J. W. Chung, S. Y. Lee and Z. Bao, *J. Am. Chem. Soc.*, 2012, **134**, 2760–2765.
37 Q. Li, J. Wu, R. Wu, Y. Liu, H. Chen, F. Huang and H. Li, *Sci. China: Chem.*, 2017, **60**, 490–496.
38 E. Orgiu, S. Locci, B. Fraboni, E. Scavetta, P. Lugli and A. Bonfiglio, *Org. Electron.*, 2011, **12**, 477–485.
39 S. Nam, H. Jeon, S. H. Kim, J. Jang, C. Yang and C. E. Park, *Org. Electron.*, 2009, **10**, 67–72.
40 L. Feng, C. Jiang, H. Ma, X. Guo and A. Nathan, *Org. Electron.*, 2016, **38**, 186–192.
41 R. Schroeder, L. A. Majewski and M. Grell, *Appl. Phys. Lett.*, 2004, **84**, 1004–1006.
42 M. Shao, S. Das, K. Xiao, J. Chen, J. K. Keum, I. N. Ivanov, G. Gu, W. Durant, D. Li and D. B. Geohegan, *J. Mater. Chem. C*, 2013, **1**, 4384–4390.
43 C. Kim, Z. Wang, H.-J. Choi, Y.-G. Ha, A. Facchetti and T. J. Marks, *J. Am. Chem. Soc.*, 2008, **130**, 6867–6878.
44 Q.-F. Li, S. Liu, H.-Z. Chen and H.-Y. Li, *Chin. Chem. Lett.*, 2016, **27**, 1421–1428.
45 S. Wang, C.-W. Leung and P. K. L. Chan, *Org. Electron.*, 2010, **11**, 990–995.
46 H. T. Lin, Z. Pei and Y. J. Chan, *IEEE Electron Device Lett.*, 2007, **28**, 569–571.
47 K. J. Baeg, Y. Y. Noh, J. Ghim, S. J. Kang, H. Lee and D. Y. Kim, *Adv. Mater.*, 2006, **18**, 3179–3183.
48 J. E. Anthony, J. S. Brooks, D. L. Eaton and S. R. Parkin, *J. Am. Chem. Soc.*, 2001, **123**, 9482–9483.
49 G. Xue, C. Fan, J. Wu, S. Liu, Y. Liu, H. Chen, H. L. Xin and H. Li, *Mater. Horiz.*, 2015, **2**, 344–349.
50 H. Li, B. C. K. Tee, G. Giri, J. W. Chung, S. Y. Lee and Z. Bao, *Adv. Mater.*, 2012, **24**, 2588–2591.
51 H. H. Choi, W. H. Lee and K. Cho, *Adv. Funct. Mater.*, 2012, **22**, 4833–4839.
52 M. Nikolka, I. Nasrallah, B. Rose, M. K. Ravva, K. Broch, A. Sadhanala, D. Harkin, J. Charmet, M. Hurhangee, A. Brown, S. Illig, P. Too, J. Jongman, I. McCulloch, J.-L. Brédas and H. Sirringhaus, *Nat. Mater.*, 2016, **16**, 356.